Maps of the Cosmos
ASP Conference Series, Vol. 216, 2005
M. Colless, L. Staveley-Smith, R. Stathakis

The Local Large-Scale Structure from HIPASS

Martin Zwaan, Martin Meyer, and Rachel Webster,

The University of Melbourne, Victoria 3010, Australia

Lister Staveley-Smith

Australia Telescope National Facility, Epping NSW 1710, Australia

and the HIPASS team

Abstract. The HI Parkes All Sky Survey (HIPASS) offers a unique perspective on the galaxy population in the local universe. A catalogue of 4315 HI-selected galaxies has been extracted from the southern region of the survey ($\delta < +2°$). This catalogue gives a clear view of the local large-scale structure and is used to study the two-point correlation function, the Tully-Fisher relation, and galaxy luminosity and mass functions. Some initial results are discussed here.

1. Introduction

In 1997 a large team of astronomers set out to survey the entire southern sky for neutral hydrogen emission (HI) using the Parkes Telescope. To blindly survey the sky for the HI 21-cm line has traditionally been very expensive in telescope time, resulting in either blind surveys of relatively small volumes (e.g. Shostak 1977; Krumm & Brosch 1984; Kerr & Henning 1987; Zwaan et al. 1997; Rosenberg & Schneider 2000), or targeted surveys across larger regions through the use of existing, typically optical, catalogues (e.g. Fisher & Tully 1981; Mathewson, Ford, & Buchhorn 1992; Giovanelli, Avera, & Karachentsev 1997). Equipped with the 21-cm multibeam receiver, the Parkes Telescope is a very efficient survey tool, which allowed us for the first time to conduct an all-sky untargeted neutral hydrogen emission line survey, simultaneously in the intermediate neighborhood of the Milky Way Galaxy, as well as in a large volume around it, out to distances of $170h_{75}^{-1}$ Mpc.

The data taking for this survey, known as HIPASS (HI Parkes All Sky Survey), was finished in 2002, and since then much effort has gone into analyzing the large data set. Here, we concentrate on some of the progress that has been made with the extragalactic component of HIPASS.

2. The HI Parkes All Sky Survey (HIPASS)

The HIPASS data consists of 530 cubes, which each cover 8 by 8 degrees on the sky, and nearly 14000 km/s in redshift space (from -1280 to 12700 km/s). Together these cubes comprise almost two thirds of the sky, from declination

-90 to +25 degrees. This survey has a per beam integration time of 450s and a velocity resolution of 18.0 km/s. Observations and data processing are described in detail in Barnes et al. (2001). So far, most attention has been directed to the 388 southern cubes south of declination 2 degrees.

The first task after creating the data cubes was to identify extragalactic neutral hydrogen 21-cm emission line signals in the noisy background. It was found that this was most efficiently done using two independent automatic finder algorithms, the results of which were merged. Galactic high velocity clouds and detections at frequencies known to be polluted by man-made interference were removed from the list of detections. The remaining potential detections were subjected to a series of manual checks for verification by three different individuals. After this process, we were left with 4,315 HI-selected galaxies, 16 times larger than any HI-selected sample prior to HIPASS. This sample of HI selected galaxies from HIPASS is referred to as HICAT.

The details of the data search, verification, and parametrization methods, along with a description of the measured quantities are described in Meyer et al. (2004). A companion paper (Zwaan et al. 2004) details the completeness and reliability of HICAT. The completeness is calculated from the recovery rate of synthetic sources that were placed in the data cubes. The reliability is determined by re-observing with the Parkes Telescope a large number of catalogue galaxies. HICAT is found to be 99% complete at a peak flux density of 84 mJy and an integrated flux of 9.4 Jy km/s. The overall reliability is 95%, but rises to 99% for sources with peak fluxes > 58 mJy.

The full catalogue data including positions, fluxes, and derived quantities, is made available to the astronomical community via `http://hipass.aus-vo.org`.

3. Large-Scale Structure

Figure 1 shows the sky distribution of the HICAT sources. The Galactic Plane is indicated by the dashed line labeled with "b=0". All optical surveys suffer from severe extinction in this region, leading to an incomplete picture of large-scale structure. However, as an HI survey, HIPASS is affected to a much smaller degree by the Galactic Plane.

Significant structure in the survey volume is observed. Features seen range from major under-dense regions in the local universe, such as the Local Void, to major over-dense regions such as the Local Supercluster (seen in projection as the Supergalactic plane, indicated by the fat solid line). With many of these structures observed uninterrupted through the Zone of Avoidance, HICAT offers new opportunities to quantify their three dimensional properties. The Local Void is observed to extend from the lowest velocities probed by HICAT to $\sim$ 6000 km/s. Comparing the two-dimensional distribution of HICAT galaxies to the locations of known groups and clusters, significant correlation is observed. Thus although over-dense regions such a galaxy clusters are not necessarily visible in HI (Waugh et al. 2002), on the largest scales optical and HI galaxy distributions align (see Meyer et al. 2003).

The clustering of HICAT galaxies is quantified through calculation of the two-point correlation function (Meyer 2003). From the HICAT redshift-space Kaiser diagram, evidence is seen for systematic trends in the peculiar velocities

https://doi.org/10.1017/S0074180900196639 Published online by Cambridge University Press

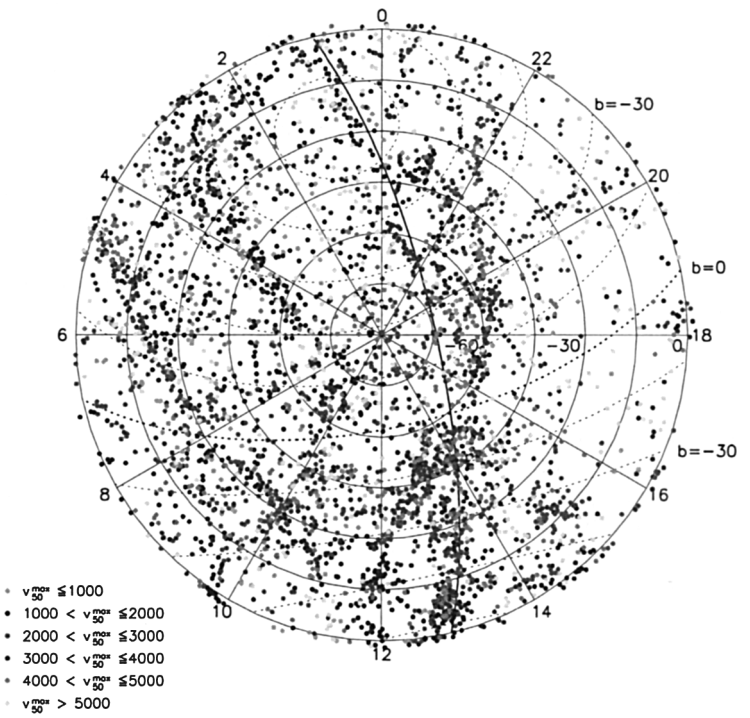

Figure 1. Polar projection of HICAT detections. Light solid lines are equatorial coordinates, the fat solid line indicates the Supergalactic plane.

of galaxies similar to those observed in the optical. These distort the two-dimensional redshift-space correlation function contours away from their true real-space values. On small scales, the peculiar velocities of galaxies in gravitationally bound concentrations stretch the redshift-space correlation function values in the radial direction. For HICAT, this is interpreted as the result of galaxy peculiar velocities in small-scale over-densities such as galaxy groups, given the relative absence of HI-rich galaxies in more over-dense environments such as galaxy clusters. On large angular scales, flattening of the two-dimensional correlation function is also observed. This is caused by the coherent in-fall of galaxies into the largest-scale filaments of the galaxy space distribution.

The real-space two-point correlation function is calculated following the procedures described by Norberg et al. (2001), and is shown in Figure 2. Also shown in this diagram is the correlation function measured from the 2dF Galaxy Redshift Survey (2dFGRS; Hawkins et al. 2003). Clearly, the HI-selected galaxies are less strongly clustered than the 2dFGRS galaxies. The clustering correlation length of HICAT galaxies is found to be $r_0 = 2.6 \pm 0.3h^{-1}$ Mpc (not weighted for sample selection function) or $r_0 = 3.2 \pm 0.4h^{-1}$ Mpc (weighted). The difference between the unweighted and weighted results is probably due to cosmic variance, with the closest regions of the universe potentially under-dense.

https://doi.org/10.1017/S0074180900196639 Published online by Cambridge University Press

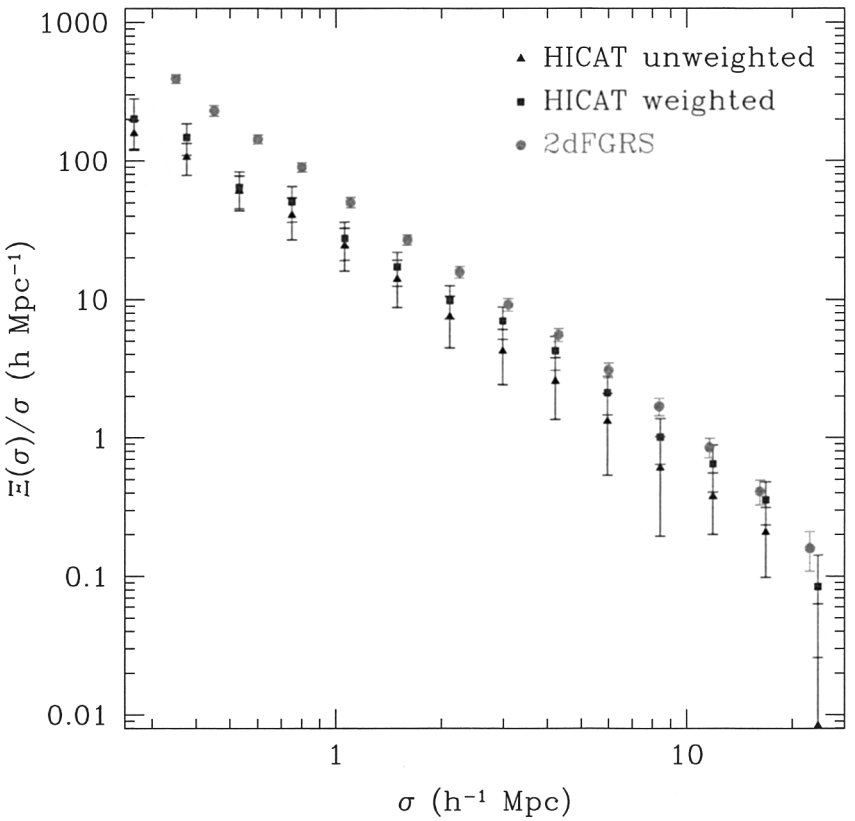

Figure 2. Projected real-space two-point correlation function for the HICAT sample (triangles: unweighted, squares: weighted) compared to the 2dFGRS results (Hawkins et al. 2003, circles). HI-selected galaxies are clearly more weakly clustered.

Interestingly, the HICAT correlation length is within the errors of the faint late-type galaxies in the 2dFGRS, consistent with known trends of HI-richness and morphology along the Hubble sequence. This is illustrated in Figure 3, where the clustering length of HICAT galaxies is compared to those of 2dFGRS galaxies of different optical luminosities. The average luminosity of HICAT galaxies is estimated from ESO-LV (Lauberts & Valentijn 1989) magnitudes. It should be noted that this average luminosity will likely overestimate the true mean luminosity of HICAT galaxies, because HICAT galaxies without ESO-LV matches will be preferentially faint. The low clustering length places HI-rich galaxies at the extreme end of the clustering distribution and makes them among the most weakly clustered objects known.

Two potential effects that cause the weaker clustering of HICAT galaxies are possibly at play here. First, HI-rich galaxies may avoid the densest regions

https://doi.org/10.1017/S0074180900196639 Published online by Cambridge University Press

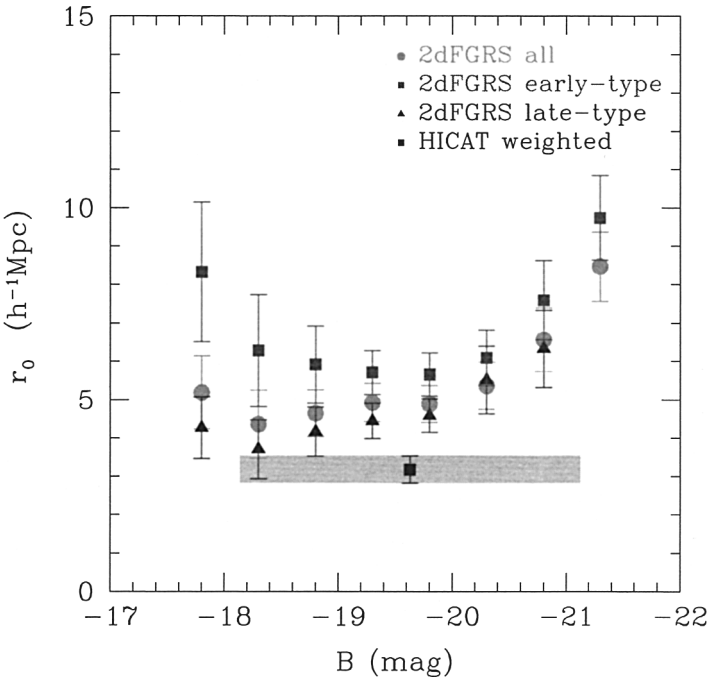

Figure 3. HICAT correlation length compared to the 2dFGRS results, plotted as a function of absolute B-band magnitude. HI-selected galaxies are the most weakly clustered objects known.

due to the depletion of HI gas by environmental processes. Potential mechanisms include tidal stripping, ram pressure stripping, the recently proposed method of strangulation, or star formation triggered by tidal interactions. Alternatively, HI-rich galaxies may actually form in the less strongly clustered halos of the initial density distribution, these corresponding to low-medium density peaks that are yet to be accreted onto the most massive systems.

4. HI Mass Function

Apart from studying the large-scale structure, HIPASS is very useful for measuring exactly how HI is distributed over galaxies of different masses. The HI mass function (or HIMF) was originally introduced by Briggs (1990), who made an estimate based on optical luminosity functions and the typical HI mass to optical luminosity ratios of galaxies. Blind HI surveys with the Arecibo Telescope resulted in the first independent measurements of the HIMF (Zwaan et al. 1997; Rosenberg & Schneider 2002), but different groups reported different values of the Schechter faint-end slope from $\alpha = -1.2$ to $\alpha = -1.5$. Now, with HICAT, the HIMF can be determined with unprecedented accuracy.

https://doi.org/10.1017/S0074180900196639 Published online by Cambridge University Press

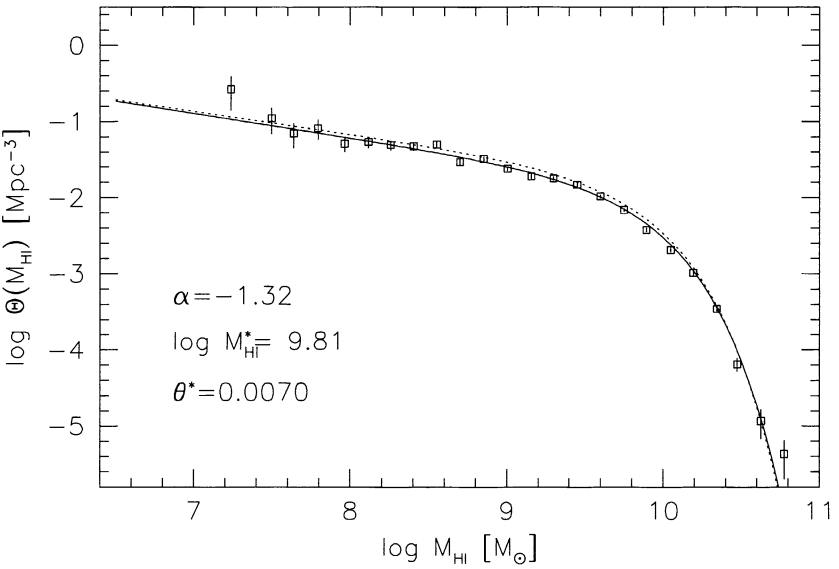

Figure 4. HI mass function from the full HIPASS catalogue of 4315 galaxies. Open squares are the maximum likelihood solutions of the space densities of galaxies, and the solid line is the best fit Schechter function with the fit-parameters indicated in the lower left corner. The dashed line shows the HIMF from the 1000 brightest HIPASS galaxies from Zwaan et al. (2003). The new measurement from the full catalogue is similar, but more accurate.

For the calculation of the HI mass function we used a bivariate maximum likelihood method, which solves for the HI mass and the velocity width simultaneously. This bivariate method finds the proper space density of galaxies, taking into account the completeness and reliability of the HICAT galaxy sample. The normalization is determined by calculating the mean galaxy density $\bar{n}$ via the minimum variance estimator (Davis & Huchra 1982) and setting $\bar{n}$ equal to the integral over the HI mass function. Only the distance range corresponding to values of the selection function S in the range $0.001 < S < 0.1$ is used in the calculation of $\bar{n}$, to avoid adding noise from the farthest and nearest regions of velocity space where the number of galaxies is low.

Figure 4 shows the HICAT HI mass function, with the best-fit Schechter parameters shown in the lower left corner. The HI mass function from the brightest 1000 HIPASS galaxies is also shown by a dashed line (Zwaan et al. 2003). Our new HI mass function is in good agreement with the earlier measurement, and allows for a precise evaluation of the neutral gas mass density at the present epoch. Expressed as a fraction of the critical density of the universe, the neutral gas mass density is only 0.038%. This is approximately five times lower than at the time when the universe was only 10% its present age (Storrie-Lombardi & Wolfe 2000), indicating the gradual conversion from neutral gas to stars in the disks of galaxies.

https://doi.org/10.1017/S0074180900196639 Published online by Cambridge University Press

References

Barnes, D. G., et al. 2001, MNRAS, 322, 486
Briggs, F. H. 1990, AJ, 100, 999
Davis, M., & Huchra, J. 1982, ApJ, 254, 437
Fisher, J. R., & Tully, R. B. 1981, ApJS, 47, 139
Giovanelli, R., Avera, E., & Karachentsev, I. D. 1997, AJ, 114, 12
Hawkins, E., et al. 2003, MNRAS, 346, 78
Kerr, F. J., & Henning, P. A. 1987, ApJL, 320, L99
Krumm, N., & Brosch, N. 1984, AJ, 89, 146
Lauberts, A., & Valentijn, E. A. 1989, The Surface Photometry Catalogue of the ESO-Uppsala Galaxies, (Garching: European Southern Observatory)
Mathewson, D. S., Ford, V. L., & Buchhorn, M. 1992, ApJS, 81, 413
Meyer, M. J. 2003, PhD Thesis, University of Melbourne
Meyer, M. J., et al. 2003, ASSL, 281, 21
Meyer, M. J., et al. 2004, MNRAS, 350, 1195
Norberg, P., et al. 2001, MNRAS, 328, 64
Rosenberg, J. L., & Schneider, S. E. 2000, ApJS, 130, 177
Rosenberg, J. L., & Schneider, S. E. 2002, ApJ, 567, 247
Shostak, G. S. 1977, AAP, 54, 919
Storrie-Lombardi, L. J., & Wolfe, A. M. 2000, ApJ, 543, 552
Waugh, M., et al. 2002, MNRAS, 337, 641
Zwaan, M. A., Briggs, F. H., Sprayberry, D., & Sorar, E. 1997, ApJ, 490, 173
Zwaan, M. A., et al. 2003, AJ, 125, 2842
Zwaan, M. A., et al. 2004, MNRAS, 350, 1210